University of Tehran Press

Pollution

Print ISSN: 2383-451X
Online ISSN: 2383-4501

https://jpoll.ut.ac.ir/

A Study on the Effects of Operating Parameters on the Degradation of Oxalic Acid in a Photocatalytic Reactor using Computational Fluid Dynamics

Lin Gao | Yuanzhen Jiang | Kaiyang Ye | Baoqing Deng✉

Department of Environmental Science and Engineering, University of Shanghai for Science and Technology, Shanghai 200093, P. R. China

Article Info

Article type:
Research Article

Article history:
Received: 28 Aug 2022
Revised: 12 Dec 2022
Accepted: 17 Jan 2023

Keywords:
Photocatalytic reactor
Photocatalytic Degradation
Computational fluid dynamics

ABSTRACT

The simulation of photocatalytic reactor is conducted using computational fluid dynamics. Turbulence is described by using the RNG k-ε turbulence model. The DO radiation model is used to simulate the irradiance distribution in the photocatalytic reactor. The effects of operating parameters on the performance of photocatalytic reactor are considered. Results show that the degradation rate of oxalic acid decreases with the increase of inlet flow. The degradation efficiency decreases from 50% to 40% when the flow rate changes from 2.5 $m^3 h^{-1}$ to 10 $m^3 h^{-1}$. The degradation rate of oxalic acid can be improved by increasing the irradiance of the lamp. The degradation efficiency of oxalic acid in the photocatalytic reactor first reaches a maximum degradation efficiency with the increase of titanium dioxide concentration, and then decreases with the increase of titanium dioxide concentration. An optimal concentration of catalysts exists. The maximum degradation efficiency is 27% for the catalyst concentration of 20 $\mu g L^{-1}$.

Cite this article: Gao, L., Jiang, Y., Ye, K., & Deng, B. (2023). A Study on the Effects of Operating Parameters on the Degradation of Oxalic Acid in a Photocatalytic Reactor using Computational Fluid Dynamics. *Pollution* , 9 (2), 579-590. http://doi.org/10.22059/POLL.2022.347830.1598

 Publisher: University of Tehran Press.
DOI: http://doi.org/10.22059/POLL.2022.347830.1598

INTRODUCTION

Photocatalytic oxidation technology has attracted widespread attention due to high oxidation capacity, good stability, low energy consumption and no secondary pollution (Klavarioti et al. 2009; Irawaty et al. 2014; Schneider et al. 2014; Fagan et al. 2016; AlSalka et al. 2018). In photocatalytic reactors, the degradation of pollutants depends on the kinetics, the distribution of light and the reactor hydrodynamics. When the catalyst and pollutant are specified, the reactor hydrodynamics plays a significant role in the performance of photocatalytic reactors.

Computational fluid dynamics (CFD) has been widely used to simulate the performance of photocatalytic reactors (Jarandehei and Visscher 2009; Mueses et al. 2013; Trujillo et al. 2010; Boyjoo et al. 2013). Qi et al. (2011) investigated the photocatalytic reaction in the reactor using CFD method. The degradation of organic pollutants was greatly affected by local hydrodynamics and light intensity. Boyjoo et al. (2014) simulated the photocatalytic process in a ring-shaped photocatalytic reactor. The results showed that CFD can be used to optimize the photocatalytic process. Casado et al. (2017) simulated the fluid dynamics, radiation transfer, mass transfer and chemical reaction rate in the photocatalytic reactor by using the CFD model. The simulation

*Corresponding Author Email: *bqdeng@usst.edu.cn*

results showed that CFD method is applicable to the design and optimization of photocatalytic reactors. Amani et al. (2018) studied the effects of operating conditions on phenol removal in a batch bioreactor. O B Lira et al. (2019) investigated the effects of relative humidity, radiation intensity, and NO concentration on photocatalytic performance in a two-dimensional reactor. Vaiano et al. (2015) carried out CFD simulation of photocatalytic degradation of methylene blue in a laboratory scale photoreactor. Long contact time can increase the methylene blue conversion. Ahmed et al. (2022) conducted a numerical and experimental study on phenol degradation in a flat plate photocatalytic reactor. The UV lamp was installed outside the flat plate photocatalytic reactor. The experimental results showed that the increasing irradiation can enhance the phenol degradation whereas the increasing initial concentration can decrease the phenol degradation. These two studies were conducted for flat plate photocatalytic reactor, which didn't interpret the influence of complex reactors.

This paper presents a detailed CFD analysis of a photocatalytic reactor with four UV lamps inside. Flow field was solved based on the RNG k-ε turbulence model. The DO radiation model was used to simulate the irradiation conditions in the photocatalytic reactor. The effects of operating conditions, including inlet flow, lamp irradiance and catalyst concentration on the performance of photocatalytic reactor are studied in detail. Both the increase in flow rate and the decrease in lamp power can lead to the decrease in degradation efficiency. An optimal catalyst concentration exists in the degradation.

MATERIALS AND METHODS

Governing equations

The flow rate and the concentration at the inlet of the photoreactor are fixed. Thus, the photoreactor is operated under steady mode (de Brito Lira et al. 2022). The transient term can be neglected in the governing equation. When the flow is turbulent, the continuity equation and the Reynolds-averaged Navier-Stokes equation can be written as follows

$$\frac{\partial u_i}{\partial x_i} = 0 \tag{1}$$

$$\frac{\partial \left(\rho u_i u_j\right)}{\partial x_j} = -\frac{\partial p}{\partial x_i} + \frac{\partial}{\partial x_j}\left(\left(\mu + \mu_t\right)\frac{\partial u_i}{\partial x_j}\right) \tag{2}$$

where u_i is the velocity component, x_i is the coordinate component, p is the pressure, ρ is the density, μ is the molecular viscosity, μ_t is the turbulent viscosity.

The turbulent viscosity can be evaluated by the turbulent kinetic energy and its dissipation rate as follows:

$$\mu_t = C_\mu \frac{k^2}{\varepsilon} \tag{3}$$

where k is the turbulent kinetic energy, ε is the dissipation rate of turbulent kinetic energy, and $C\mu$ is a constant. The RNG $k - \varepsilon$ turbulence model is used to solve the turbulent kinetic energy and its dissipation rate

$$\frac{\partial \left(\rho u_j k\right)}{\partial x_j} = \frac{\partial}{\partial x_j}\left[\alpha_k \left(\mu + \mu_t\right)\frac{\partial k}{\partial x_j}\right] + G_k - \rho\varepsilon \tag{4}$$

$$\frac{\partial\left(\rho u_j \varepsilon\right)}{\partial x_j}=\frac{\partial}{\partial x_j}\left[\alpha_\varepsilon\left(\mu+\mu_t\right)\frac{\partial \varepsilon}{\partial x_j}\right]+C_{\varepsilon 1}\frac{\varepsilon}{k}G_k-C_{\varepsilon 2}\rho\frac{\varepsilon^2}{k} \tag{5}$$

where α_k is the inverse effective Prandtl number for k, α_ε is the inverse effective Prandtl number ε, G_k represents the generation from the averaged velocity gradient. The RNG model can reproduce the recirculation zone in the reactor (Saeed et al. 2017, Perez-Herrera et al. 2022). The standard wall function is used for the near-wall treatment (Wang et al. 2006).

The transport of pollutant is governed by the advection-diffusion-reaction equation, which reads

$$\frac{\partial\left(\rho u_j C\right)}{\partial x_j}=\frac{\partial}{\partial x_j}\left[\left(\mu+\frac{\mu_t}{Sc_t}\right)\frac{\partial C}{\partial x_j}\right]+S_C \tag{6}$$

where C is the concentration of the pollutant, Sc stands for the destruction term of the pollutant, Sc_t is the turbulent Schmidt number. Oxalic acid is selected as a model pollutant. Following Salvad´o-Estivill et al. (2007), the destruction term of oxalic acid can be evaluated by the rate equation

$$S_c=-\left\{k_B\theta(t)C+k_A\left[1-\theta(t)\sqrt{C}\right]\right\}\sqrt{LVRPA} \tag{7}$$

with

$$\theta(t)=\beta C_{in}\left(1-\alpha t LVRPA\right) \tag{8}$$

where LVRPA is the local volumetric rate of photon absorption, which writes

$$LVRPA=a\int_0^{4\pi} I\left(\vec{r},\vec{s}\right)d\Omega \tag{9}$$

where a is the absorption coefficient of light in the medium, I is the radiation intensity. The solution of LVRPA requires the light intensity within the photoreactor. The radiative transfer equation (RTE) is used to solve the light intensity, which describes the electromagnetic wave propagation through the medium

$$\frac{dI(\vec{r},\vec{s})}{ds}+\left(a(\vec{r})+\sigma_s(\vec{r})\right)I(\vec{r},\vec{s})=\frac{\sigma_s(\vec{r})}{4\pi}\int_0^{4\pi} I\left(\vec{r},\overrightarrow{s'}\right)\Phi\left(\vec{s}\cdot\overrightarrow{s'}\right)d\Omega \tag{10}$$

where $\vec{r}$ is the position vector, $\vec{s}$ is the direction vector, n is the refractive index, σs is the scattering coefficient, σ is the Stefan-Boltzmann constant, T is the local temperature, Φ is the phase function.

Numerical simulation

A cylindrical photocatalytic reactor with a length of 0.3 m and a diameter of 0.15 m is simulated, as shown in Fig. 1. Four ultraviolet lamps with a length of 0.3 m and a diameter

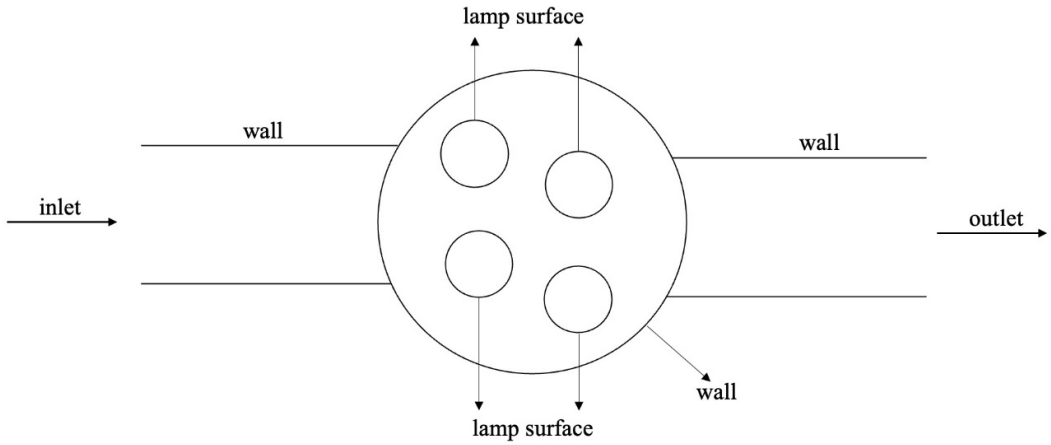

Fig. 1. Structure of photocatalytic reactor reaction chamber

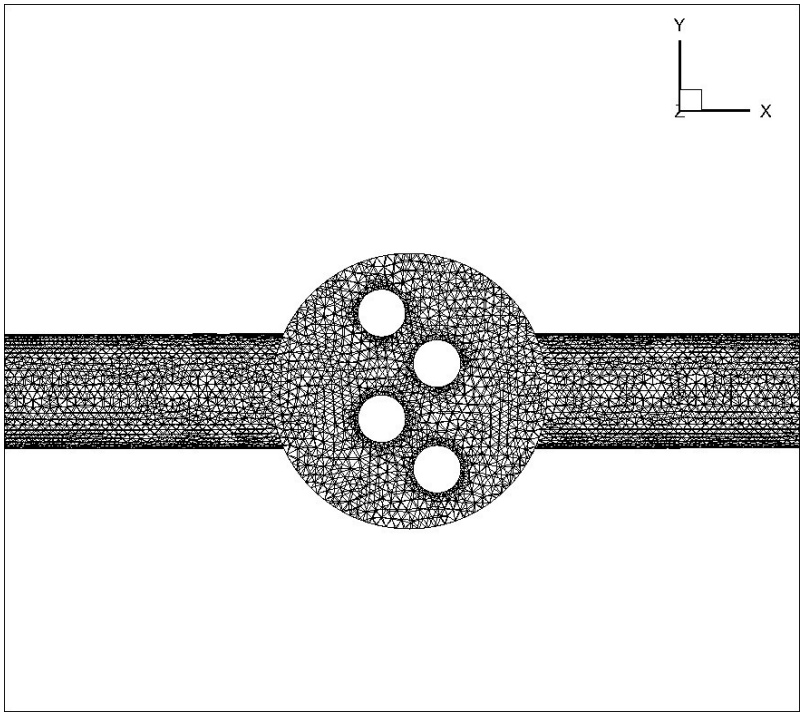

Fig. 2. Schematic of grid

of 0.052 m are installed perpendicular to the flow direction in the reactor. The surface area of ultraviolet lamp is 0.025 m^2, and the irradiance of the lamp is 700 Wm^{-2}. The slurry with titanium dioxide suspension flows into the reactor. Under the irradiation of UV light, pollutants are oxidized.

The computational domain is discretized into the tetrahedral grid using ANSYS ICEM, as shown in Fig. 2. The number of cells is 698,754. The inlet and outlet are extended to upstream and downstream for the specification of boundary conditions. Grid is refined near UV lamps and reactor walls. All governing equations are discretized using the finite volume method and solved

using ANSYS Fluent. The SIMPLE algorithm is used to treat the pressure-velocity coupling. All convection terms are discretized with second-order upwind differencing scheme. The radiative transfer equation is solved by using the discrete ordinates model. The theta and phi divisions are 5×5 and the theta and phi pixels are 3×3. The residual criteria are 1.0×10^{-4} for the momentum equation and 1.0×10^{-6} for the concentration and the radiative transfer equation.

No slip condition is adopted at all walls. The standard wall function is used to bridge between the wall and core turbulence region. No pollutant can penetrate through the wall. The velocity and the concentration are specified at the inlet. Three flow rates are considered. The fully developed flow is assumed at the outlet. Water is the medium in the photocatalytic reactor. The absorption coefficient is 5.9 m^{-1}, the scattering coefficient is 29.3 m^{-1} and the refraction index is 1.38. The diffuse reflectance of the reactor wall is unity. Lamp surface is semi-transparent and the diffuse fraction is unity. Three lamp powers are used to simulate the radiation intensity in the reactor. The turbulent Schmidt number σ_C is 0.7.

Grid sensitivity analysis is conducted for grid 1 (534,423 cells), grid 2 (698,754 cells) and grid 3 (1,021,782 cells). As shown in Fig. 3, the velocity and the turbulent viscosity are close each other for grid 1 and grid 2. Thus, the present 698,754 cells can achieve satisfactory results.

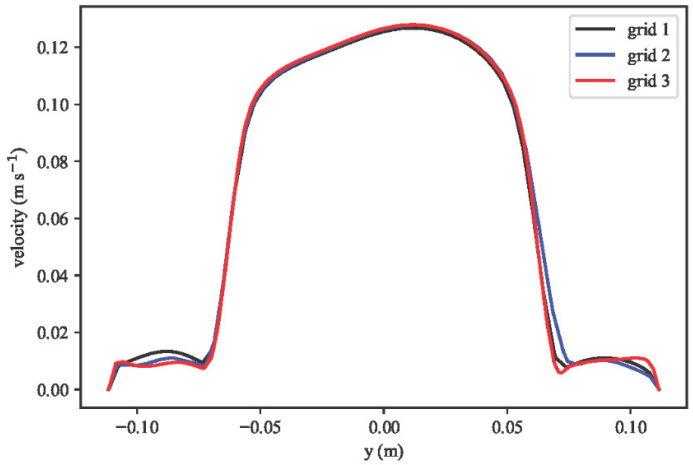

(a) velocity

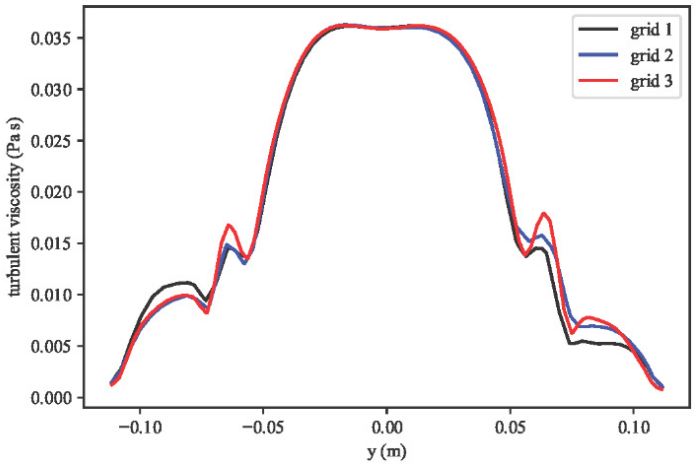

Fig. 3. Grid sensitivity

RESULTS AND DISCUSSION

Fig. 4 shows the simulated velocity at two lines. The experimental data of Wols et al. (2010) is also included in the figure. Line 1 is in front of four lamps and Line 2 is behind four lamps. In general, the simulated velocity is in good agreement with the experimental data.

Fig. 5 illustrates the distribution of radiation intensity in the plane of z = 0.075 m in the

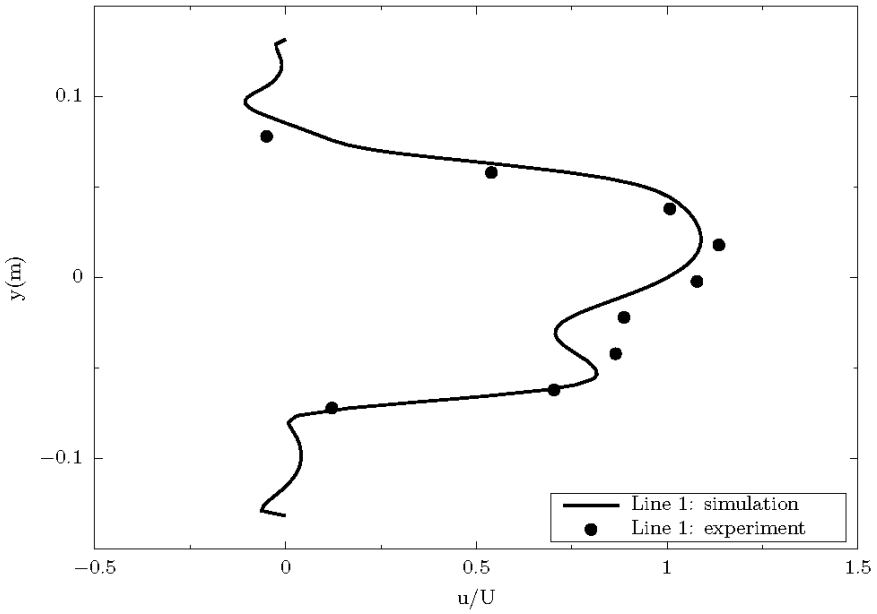

(a) Line 1

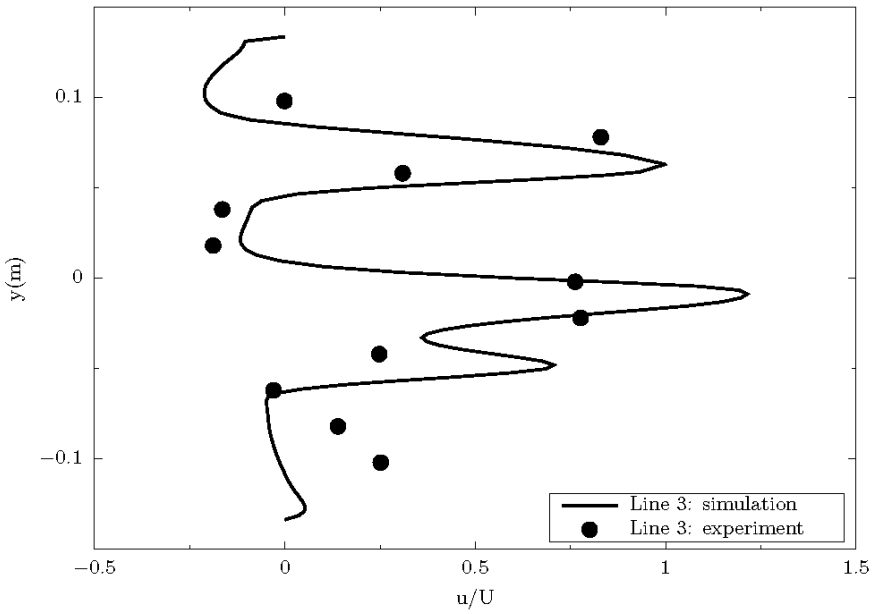

(b) Line 3

Fig. 4. Comparison of simulated velocity and the experimental data

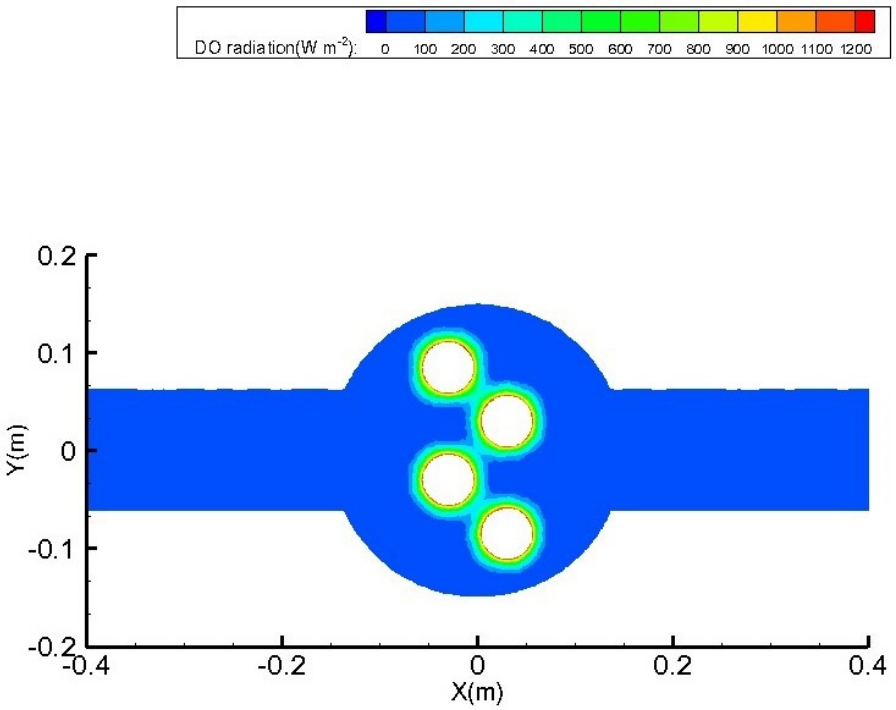

Fig. 5. Radiation distribution in the plane of z = 0.075 m

photocatalytic reactor. The maximum light intensity at the surface of UV lamps is around 1200 Wm^{-2}. The radiation depicts a circle pattern around the lamp center. With the increase of the distance from the lamp, the radiation intensity decreases rapidly. The radiation intensity in the intersection region of UV lamps is not augmented, meaning the interaction between UV lamps is weak. This phenomenon is caused by the relative long distance between lamps.

Fig. 6 shows the concentration in the plane of z = 0.075 m for different flow rates. There exists an asymmetric pattern in the concentration distribution. The ratio of concentration of oxalic acid in the top part of the reaction chamber to the inlet concentration is about 10% for the flow rate of 2.5 $m^3 h^{-1}$, 20% for the flow rate of 5 $m^3 h^{-1}$ and 30% for the flow rate of 10 $m^3 h^{-1}$. The ratio of concentration of oxalic acid in the bottom part of the reaction chamber to the inlet concentration is about 40% for the flow rate of 2.5 $m^3 h^{-1}$, 40% for the flow rate of 5 $m^3 h^{-1}$ and 50% for the flow rate of 10 $m^3 h^{-1}$. This phenomenon is due to the positions of UV lamps, which restricts the flow in the top part and prolongs the residence of pollutants in the top part of the chamber. The ratio of the outlet concentration of oxalic acid to the inlet concentration is 0.178 for the flow rate of 2.5 $m^3 h^{-1}$, 0.27 for the flow rate of 5 $m^3 h^{-1}$ and 0.641 for the flow rate of 10 $m^3 h^{-1}$. Small flow rate offers a larger residence time in the reaction chamber such that oxalic acid can be oxidized sufficiently. The decrease in photocatalytic efficiency due to the increase in flow rates were also found in literature (Vaiano et al. 2015, Ahmed et al. 2022)

Fig. 7 depicts the distribution of concentration for different lamp irradiance. Oxalic acid near the surface of the lamp is decomposed better because most light is concentrated on the lamp. The degradation efficiency of oxalic acid is highest between the wall surface and the UV lamp. However, in the bottom area at the entrance of the reaction chamber, the concentration of oxalic acid is high, and its degradation effect is not good. The ratios of the concentration of oxalic acid at the outlet of the reaction chamber to the inlet concentration at the three different

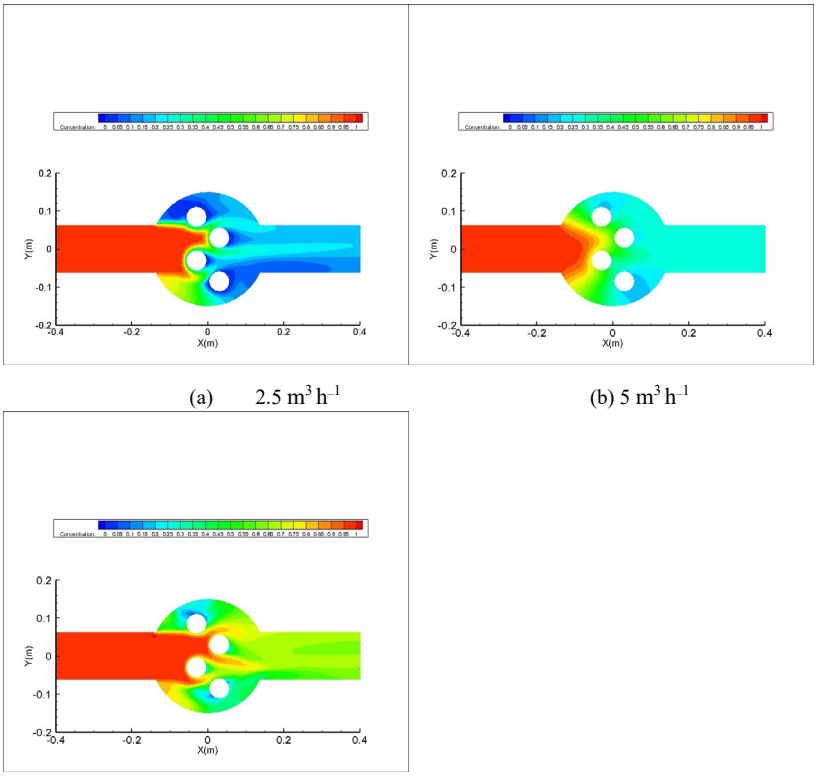

(a) 2.5 $m^3 h^{-1}$ (b) 5 $m^3 h^{-1}$

(c) 10 $m^3 h^{-1}$

Fig. 6. The concentration of oxalic acid in the plane of z = 0.075 m under different flow rates

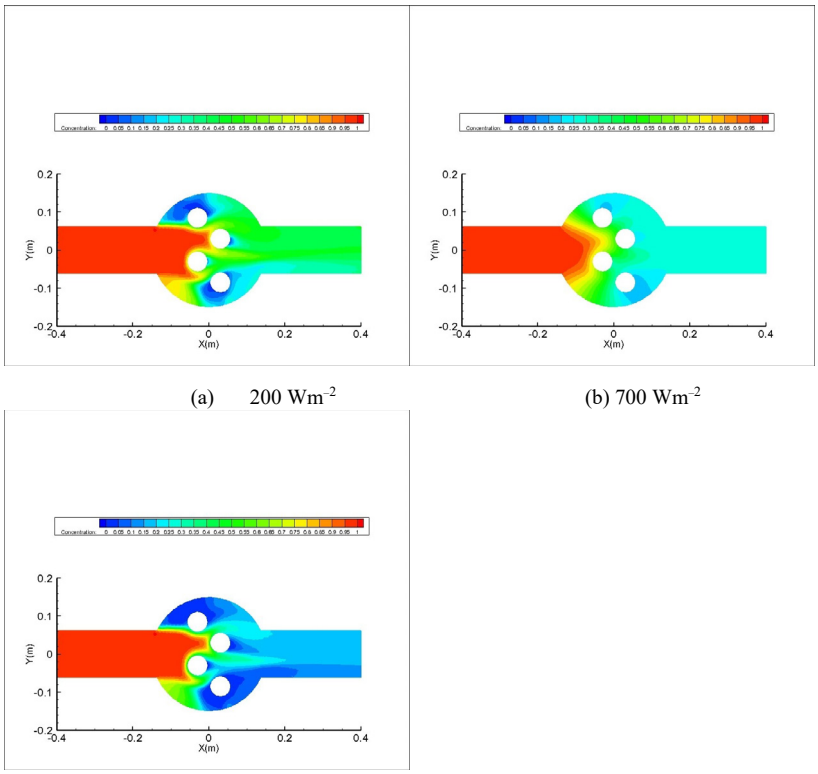

(a) 200 Wm^{-2} (b) 700 Wm^{-2}

(c)1000 Wm^{-2}

Fig. 7. The concentration of oxalic acid in the plane of z = 0.075 m for different irradiance

lamp irradiation levels are about 0.437, 0.27 and 0.177. The photocatalytic degradation can be enhanced with increasing lamp power, which was concluded in Ahmed et al. (2022).

Fig. 8 shows the distribution of concentration under different catalyst concentrations. The inlet oxalic acid concentration in the reactor is 0.9 μgL^{-1}, the inlet flow rate is 5 m^3 h^{-1}, the UV

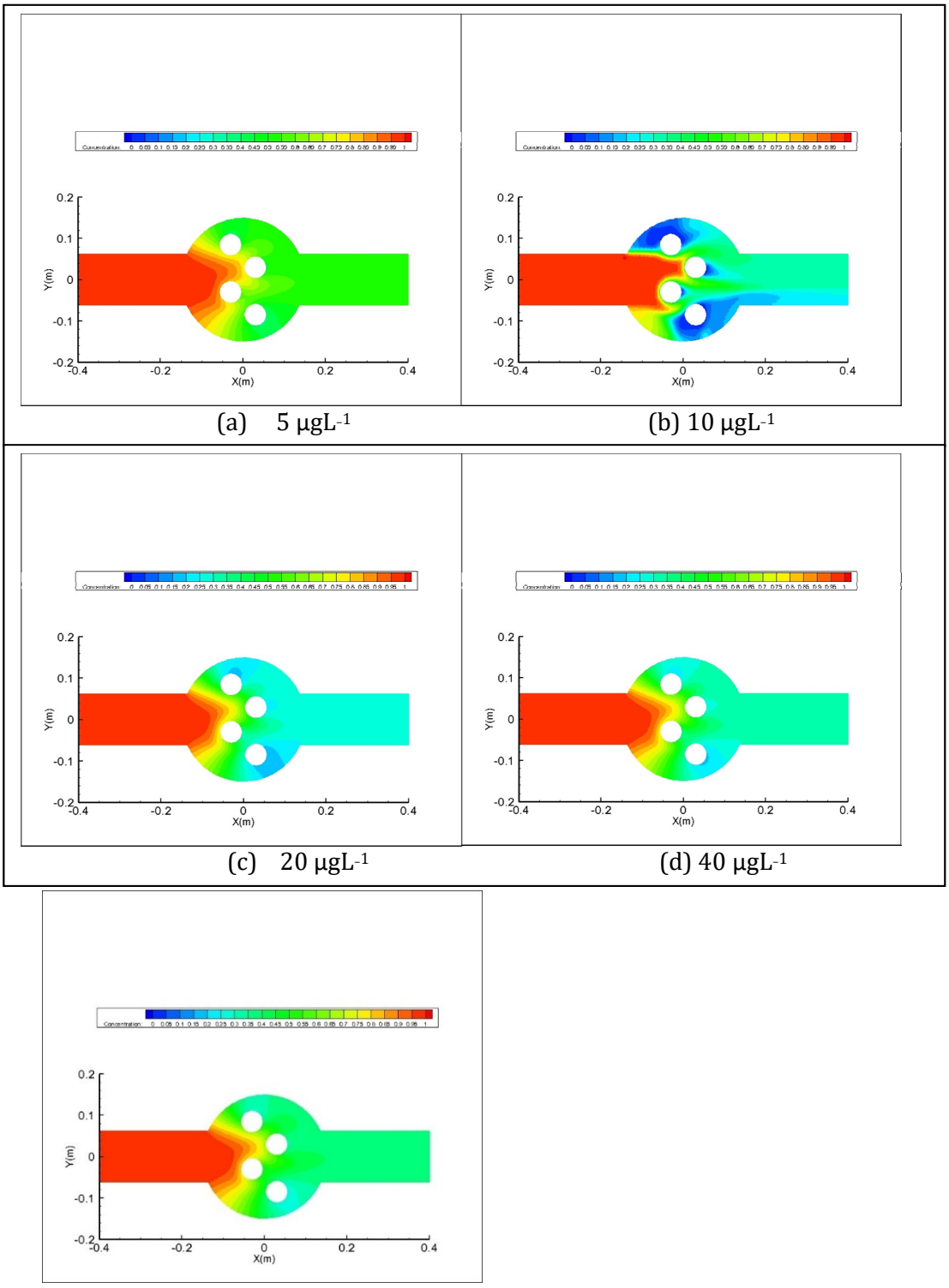

Fig. 8. The concentration of oxalic acid at z = 0.075 m for different catalyst load

lamp irradiance is 700 Wm^{-2}. The concentration of titanium dioxide has a significant effect on the degradation of oxalic acid. The ratio of the concentration of oxalic acid at the outlet of the reactor to the inlet concentration is 0.539 for the catalyst concentration of 5 μgL^{-1}, 0.319 for the catalyst concentration of 10 μgL^{-1}, 0.27 for the catalyst concentration of 20 μgL^{-1}, 0.32 for the catalyst concentration of 40 μgL^{-1} and 0.394 for the catalyst concentration of 80 μgL^{-1}. The degradation efficiency of oxalic acid increases for low values of catalyst concentration, reaches a maximum value at some catalyst concentration and then decreases with the increase in catalyst concentration. The phenomenon is due to the two-fold effect of catalyst (Wang et al. 2019). More catalyst can provide more sites for reaction, whereas more catalyst will absorb more light, decreasing the light intensity in the reaction chamber. The combined effect of these two factors leads to the existence of an optimal catalyst concentration for photocatalytic reaction. Mehrotra et al. (2005) conducted the experiment on photocatalytic degradation of benzoic acid in a slurry reactor, which verify the conclusion of present study.

CONCLUSION

A detailed CFD simulation is conducted for the photocatalytic oxidation of oxalic acid in a photocatalytic reactor. All governing equations are solved using ANSYS Fluent. The simulated velocity is validated against the experimental data in the literature. The effects of several factors on the degradation of oxalic acid in photocatalytic converters are studied. The main conclusions are listed as follows:

1) The degradation efficiency of oxalic acid in the photocatalytic reactor decreases with the increase in flow rates, changing from 50% to 40% when the flow rate changes from 2.5 $m^3 h^{-1}$ to 10 $m^3 h^{-1}$.

2) The degradation efficiency of oxalic acid in the photocatalytic reactor increases with the increase in lamp power. The outlet concentration reduces to nearly 60% when lamp power increases from 200 W m^{-2} to 1000 W m^{-2}.

3) The effect of the catalyst on the photocatalytic degradation is complex. There exists an optimal catalyst concentration that can obtain the maximum degradation efficiency. With the increase in the catalyst concentration, the degradation efficiency increases before the optimal catalyst concentration and decreases after the optimal catalyst concentration.

GRANT SUPPORT DETAILS

The authors would like to thank the financial support by Natural Science Foundation of Shanghai (No. 17ZR1419200).

CONFLICT OF INTEREST

The authors declare that there is not any conflict of interests regarding the publication of this manuscript. In addition, the ethical issues, including plagiarism, informed consent, misconduct, data fabrication and/ or falsification, double publication and/or submission, and redundancy has been completely observed by the authors.

LIFE SCIENCE REPORTING

No life science threat was practiced in this research.

REFERENCES

Ahmed, S., Rasul, M. G., Sattar, M. A. and Jahirul, M. I. (2022). Phenol degradation of waste and stormwater on a flat plate photocatalytic reactor with TiO2 on glass slide: An experimental and modelling investigation. J Water Process Eng, 47, 102769.

AlSalka, Y., Hakki, A., Fleisch, M. and Bahnemann, D. W. (2018). Understanding the degradation pathways of oxalic acid in different photocatalytic systems: Towards simultaneous photocatalytic hydrogen evolution. J Photochem Photobiol, A, 366, 81–90.

Amani, A., Jalilnejad, E. and Mousavi, S. M. (2018). Simulation of phenol biodegradation by Ralstonia eutropha in a packed-bed bioreactor with batch recycle mode using CFD technique. J Ind Eng Chem, 59, 310–319.

Boyjoo, Y., Ang, M. and Pareek, V. (2013). Light intensity distribution in multi-lamp photocatalytic reactors. Chem Eng Sci, 93, 11–21.

Boyjoo, Y., Ang, M. and Pareek, V. (2014). CFD simulation of a pilot scale slurry photocatalytic reactor and design of multiple-lamp reactors. Chem Eng Sci, 111, 266–277.

Casado, C., Marugán, J., Timmers, R., Muñoz, M. and van Grieken, R. (2017). Comprehensive multiphysics modeling of photocatalytic processes by computational fluid dynamics based on intrinsic kinetic parameters determined in a differential photoreactor. Chem Eng J, 310, 368–380.

de Brito Lira, J. O., Riella, G. H., Padoin, N. and Soares, C. (2022). Fluid dynamics and mass transfer in curved reactors: A CFD study on Dean flow effects. J Environ Chem Eng, 10, 108304.

Fagan, R., McCormack, D. E., Dionysiou, D. D. and Pillai, S. C. (2016). A review of solar and visible light active TiO2 photocatalysis for treating bacteria, cyanotoxins and contaminants of emerging concern. Mater Sci Semicond Process, 42, 2–14.

Irawaty, W., Soetaredjo, F. E. and Ayucitra, A. (2014). Understanding the Relationship between Organic Structure and Mineralization Rate of TiO2-mediated Photocatalysis. Procedia Chem, 9, 131–138.

Jarandehei, A. and De Visscher, A. (2009). Three-dimensional CFD model for a flat plate photocatalytic reactor: Degradation of TCE in a serpentine flow field. AIChE J, 55 (2), 312–320.

Klavarioti, M., Mantzavinos, D. and Kassinos, D. (2009). Removal of residual pharmaceuticals from aqueous systems by advanced oxidation processes. Environ Int, 35 (2), 402–417.

Mehrotra, K., Yablonsky, G. S. and Ray, A. K. (2005). Macro kinetic studies for photocatalytic degradation of benzoic acid in immobilized systems. Chemosphere, 60 (10), 1427–1436.

Mueses, M. A., Machuca-Martinez, F. and Li Puma, G. (2013). Effective quantum yield and reaction rate model for evaluation of photocatalytic degradation of water contaminants in heterogeneous pilot-scale solar photoreactors. Chem Eng J, 215-216, 937–947.

de OB Lira, J., Padoin, N., Vilar, V. J. and Soares, C. (2019). Photocatalytic NOx abatement: Mathematical modeling, CFD validation and reactor analysis. J Hazard Mater, 372, 145-153.

Perez-Herrera, R., de Souza, T. A., Coronado, C. J., do Nascimento, M. A. R. and Pinto, G. M. (2022). Numerical CFD Simulation of a Horizontal Cyclonic Combustion Chamber for Burning Pulverized Biomass Solid Fuels. Waste Biomass Valorization, 1-29.

Qi, N., Zhang, H., Jin, B. and Zhang, K. (2011). CFD modelling of hydrodynamics and degradation kinetics in an annular slurry photocatalytic reactor for wastewater treatment. Chem Eng J, 172 (1), 84–95.

Saeed, M., Yu, J. Y., Abdalla, A. A. A., Zhong, X. P. and Ghazanfar, M. A. (2017). An assessment of k-ε turbulence models for gas distribution analysis. Nucl Sci Tech, 28(10), 1-8.

Salvadó-Estivill, I., Hargreaves, D. M. and Li Puma, G. (2007). Evaluation of the intrinsic photocatalytic oxidation kinetics of indoor air pollutants. Environ Sci Technol, 41(6), 2028-2035.

Schneider, J., Matsuoka, M., Takeuchi, M., Zhang, J., Horiuchi, Y., Anpo, M. and Bahnemann, D. W. (2014). Understanding TiO2 photocatalysis: mechanisms and materials. Chem Rev, 114 (19), 9919–9986.

Trujillo, F. J., Safinski, T. and Adesina, A. A. (2010). Oxidative Photomineralization of Dichloroacetic Acid in an Externally-Irradiated Rectangular Bubble Tank Reactor: Computational Fluid Dynamics Modeling and Experimental Verification Studies. Ind Eng Chem Res, 49(15), 6722–6734.

Vaiano, V., Sacco, O., Pisano, D., Sannino, D. and Ciambelli, P. (2015). From the design to the development of a continuous fixed bed photoreactor for photocatalytic degradation of organic pollutants in wastewater. Chem Eng Sci, 137, 152-160.

Wang, J., Deng, B. Q., Gao, J. and Cao, H. C. (2019). Numerical simulation of radiation distribution in a

slurry reactor: The effect of distribution of catalyst particles. Chem Eng J, 357, 169-179.
Wang, J., Priestman, G. H. and Tippetts, J. R. (2006). Modelling of strongly swirling flows in a complex geometry using unstructured meshes. Int J Numer Methods Heat Fluid Flow, 16(8), 910-926.
Wols, B. A., Shao, L., Uijttewaal, W., Hofman, J., Rietveld, L. C. and van Dijk, J. C. (2010). Evaluation of experimental techniques to validate numerical computations of the hydraulics inside a UV bench-scale reactor. Chem Eng Sci, 65 (15), 4491–4502.